# Observation of the Effect of Energetic Ions on Pellet Ablation in the Large Helical Device

Mitsuyasu HOSHINO, Ryuichi SAKAMOTO[1)], Hiroshi YAMADA[1,2)], Tokihiko TOKUZAWA[1)], Kazumichi NARIHARA[1)], Masaki OSAKABE[1)], Hisayoshi FUNABA[1)], Ryuhei KUMAZAWA[1)], Tetsuo WATARI[1)] and the LHD Experimental Group[1)]

*Department of Energy Engineering and Science, Nagoya University, Nagoya 464-8603, Japan*
*[1)]National Institute for Fusion Science, Toki 509-5292, Japan*
*[2)]The Graduate University for Advanced Studies, SOKENDAI, Hayama 240-0193, Japan*

(Received 10 January 2006 / Accepted 24 April 2006)

Ablation of a solid hydrogen pellet in hot plasmas was investigated in the Large Helical Device (LHD). The penetration depth of the injected pellets in the experiment was compared to a theoretical model employing ablation due to the heat flux of fast ions as well as thermal electrons. Shallower penetration than that predicted based on the model considering only electrons was observed in LHD plasmas in the presence of highly energetic (up to 180 keV) fast ions due to neutral beam injection (NBI). This discrepancy can be quantified by the contribution of fast ions in terms of the stored energy of fast ions. The ablation model calculation taking into consideration the effect of thermal electrons and fast ions agrees with the experimental results obtained by LHD. Scaling which includes the fast-ion effect on penetration depth in LHD was compared with the wider multi-experiment database (IPADBASE) [L.R. Baylor *et al.*, Nucl. Fusion **37**, 445 (1997)].



Keywords: fueling, ablation of solid hydrogen, neutral gas shielding model, fast ions, LHD, IPADBASE

DOI: 10.1585/pfr.1.033

## 1. Introduction

The establishment of an efficient fueling scenario is a principal issue in the implementation of a future magnetic fusion reactor. Degradation of fueling efficiency results in excess neural gas, which causes enhanced charge exchange loss and consequent sputtering, as well as confinement deterioration. This loss of fueling efficiency also requires a large pumping capability and increases the tritium inventory. To date, gas puffing has been successfully used as a fundamental fueling tool. However, in larger devices there is a concern regarding the worsening of the fueling efficiency of gas puffing because most fueled gas is ionized in a hot and thick scrape-off layer before it penetrates the confinement region. Therefore, the feasibility and inevitability of gas puffing in a fusion reactor is not necessarily assured.

The injection of cryogenic solid pellets, which is an alternative approach to fueling, has been attracting interest because of its advantage of deeper and more efficient fueling than gas puffing (see Review Paper [1]). Many experiments support the promise of pellet injection due to its direct fueling into the plasma core region beyond the scrap-off layer of a fusion reactor. Accumulated experimental observations have shown that the fueling efficiency of pellet injection improves with penetration depth [2–4]. Here it should be pointed out that the penetration depth of pellets involves two stages of dynamics. The first stage is the penetration of solid pellets into hot plasmas. Pellets ablate due to heat flux from the plasma and leave their mass along their trajectory. The second stage is the prompt drift of ablated high density plasmoid, which is supposed to link with a gradient of the magnetic field and gives a substantial mass deposition [5–7]. Therefore, for the prediction of fueling performance it is necessary to clarify the physical mechanisms in these two stages, i.e., the ablation process of pellets and the subsequent drift motion of the ablated plasmoid.

Since the aforementioned processes can be considered separately, the penetration depth determined by the ablation process is a primary issue in fueling. This allows the discussion of drift motion as a secondary problem. With respect to the ablation process, the neutral gas shielding (NGS) model [8, 9], which estimates heat flux due to thermal electrons and evaluates the shielding effect of ablated neutral gas against it, has been widely accepted as a standard model for explaining the results of tokamak experiments. A study of the international pellet ablation database (IPADBASE) has indicated that the penetration depths in the different devices follows regression scaling whose expression is similar to NGS scaling under the condition of scatter in the scaling data of ohmic, NBI, and ICRH plasmas [10]. An effect of fast ions on the ablation can be a potential cause of this scattering.

In contrast to electrons, the effect of energetic ions on

*author's e-mail: hoshino@nifs.ac.jp*

ablation is supposed to be much less significant because of the larger shielding effect of the ablated cloud. Although a variety of models which account for the effects of energetic ions has been proposed, experimental studies on those effects, at least systematic studies, have not yet been reported and the validity of the proposed model has not been confirmed. This is due to the lack of availability of an experimental condition which contains a large amount of energetic ions. Recently, a sophisticated ablation model that describes the interaction of a pellet with energetic ions and electrons in ICRH and LHCD experiments has been reported [11]. However, the current experimental documentation of the effect of fast ions is insufficient.

In D-T fusion reactor conditions, alpha particles with an energy of 3.5 MeV account for several percent of all ions in burning plasmas. Therefore, verification of the ablation model including the effect of energetic ions is a prerequisite for predicting the penetration depth in fusion plasmas.

The Large Helical Device (LHD) [12], which is a large-scale heliotron device, employs negative ion-based neutral beam injection (NBI) with an accelerating voltage of 180 keV (the proton ratio is 100 % since the NBI employs a negative ion source) [13]. This is in contrast to the fact that major tokamaks utilize NBI with an energy of at most 100 keV. Since pellet injection is routinely available in LHD [14, 15], an experimental study of the penetration depth of pellets in NBI heated plasmas in LHD can make a unique contribution to our understanding of the pellet ablation mechanism, in particular the effect of energetic ions over a wide energy range. In this article, we describe experimental observations of pellet penetration depth, reflecting information regarding pellet ablation in plasmas which are rich in energetic ions. We compare these observations with the results of a theoretical model. Based on available understanding derived from experimental study using LHD, tokamak data described in the IPADBASE are reconsidered with emphasis on the effect of energetic ions.

# 2. Ablation Model

## 2.1 The NGS ablation model

The neutral gas shielding (NGS) model [8, 9] is a simple theoretical model describing pellet ablation in high temperature plasmas. A neutral shielding cloud around the pellet is formed by the incident energy flux from a background plasma and assumes a steady state and shock-free transonic flow which is continuously accelerated to supersonic flow. The 1-D spherically symmetric hydrodynamic model of the expansion in the ablation cloud is then solved in the model. Only the thermal electron as mono-energetic incident particles is regarded in pellet ablation since plasma electrons dominate the cloud heating and ionization, consequently the ablation of the pellet in the model [1]. By assuming the continuous loss of mono-energetic electrons in the ablation cloud, the energy-dependent loss function $L(E)$, which is a semi-empirical formula [16], is defined as $\mathrm{d}E/\mathrm{d}r = \rho_{\mathrm{cloud}} L(E)/m$, where $m$ and $\rho_{\mathrm{cloud}}$ are the average molecular mass and the mass density of the cloud, respectively. In this model, the recession speed of the pellet surface is given by the form of simple scaling laws [9]

$$\mathrm{d}r_{\mathrm{pel}}/\mathrm{d}t \propto r_{\mathrm{pel}}^{-2/3} n_{\mathrm{e}\infty}^{1/3} T_{\mathrm{e}\infty}^{1.64}, \tag{1}$$

where $r_{\mathrm{pel}}$, $n_{\mathrm{e}\infty}$, and $T_{\mathrm{e}\infty}$ are the equivalent spherical pellet radius, the background electron density, and temperature, respectively.

## 2.2 Impact of energetic ions on pellet ablation

Only the thermal effect of electrons on pellet ablation is considered in the original NGS ablation model [8, 9]. However, the extra-thermal effect (involving fast ions and energetic electrons, etc.) should be taken into account in order to understand pellet ablation in terms of the interaction with energetic particles in a hot plasma. In Refs. [17–19], the effect of fast ions on ablation has been well studied both experimentally and theoretically. The effect of thermal ions and alpha particles on pellet ablation must also be quantified for a future fusion reactor. In this section, the contribution of energetic ions to pellet ablation is estimated while that of thermal electrons is still predominant.

In the theoretical ablation models, the rate of the contribution of energetic particles to pellet ablation is estimated using a simple formula [17, 19, 20]. The heat source in the cloud due to thermal electrons and fast particles $W = (f_{\mathrm{B}}/m)q\Lambda$ $[\mathrm{eV} \cdot \mathrm{kg}^{-1} \cdot \mathrm{s}^{-1}]$ can be an effective indicator, where $f_{\mathrm{B}}$ is the fraction of the heat flux due to electrons and fast ions. It is assumed that these fractions are uniform in the cloud, $f_{\mathrm{Be}} \approx 0.6$ on electrons and $f_{\mathrm{Bf}} \approx 1.0$ on fast ions, where they are determined by the effects of both the atomic processes and that of the geometry of the flux incidence. As well, $m$, $q$ $[\mathrm{eV} \cdot \mathrm{m}^{-2} \cdot \mathrm{s}^{-1}]$, and $\Lambda$ $[\mathrm{m}^2]$ are the average molecular mass, the heat flux to the pellet, and the effective cross-section for heat flux loss in the shielding cloud, respectively. For the heat flux $q$, the distribution function of incident thermal electrons and ions assumes a Maxwellian ($n$, $T$ and $E = 2T$ are density, temperature and energy, respectively) and those of fast particles are given by using a Fokker-Planck code as follows:

$$q_{\mathrm{e,i}\infty} = \frac{1}{2}\sqrt{\frac{e}{\pi m_{\mathrm{e,i}}}} n_{\mathrm{e,i}\infty} E_{\mathrm{e,i}\infty}^{3/2}, \tag{2}$$

$$q_{\mathrm{f},\alpha\infty} = \frac{\pi m_{\mathrm{f},\alpha}}{2e}\int_0^\infty v^5 f(v)\mathrm{d}v, \tag{3}$$

$$f(v) = \begin{cases} \dfrac{S\,\tau_{\mathrm{slowdown}}}{4\pi(v^3 + v_{\mathrm{c}}^3)} & \text{for } v > v(t) \\ 0 & \text{for } v < v(t), \end{cases} \tag{4}$$

where $m_{\mathrm{e,i}}$, $m_{\mathrm{f},\alpha}$, $S$ $[\mathrm{m}^{-3} \cdot \mathrm{s}^{-1}]$, $\tau_{\mathrm{slowdown}}$, $v_c$ and $v(t)$ are the mass of incident particles, the particle source for fast particles, the slowing-down time, the critical velocity, and the

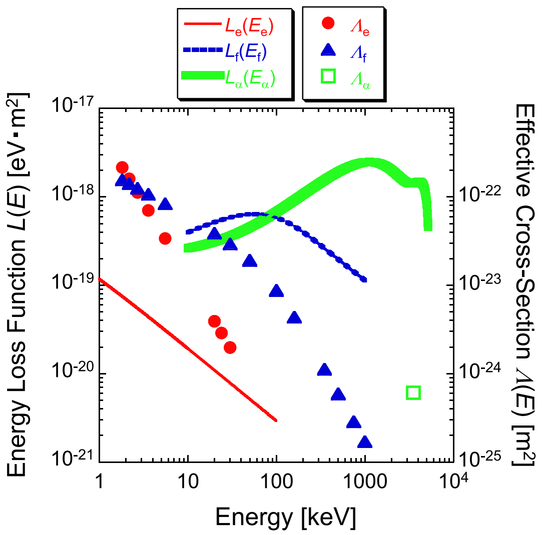


Fig. 1 Energy loss function $L(E)$ and the effective cross-section $\Lambda(E)$ of electrons, fast ions, and alphas.

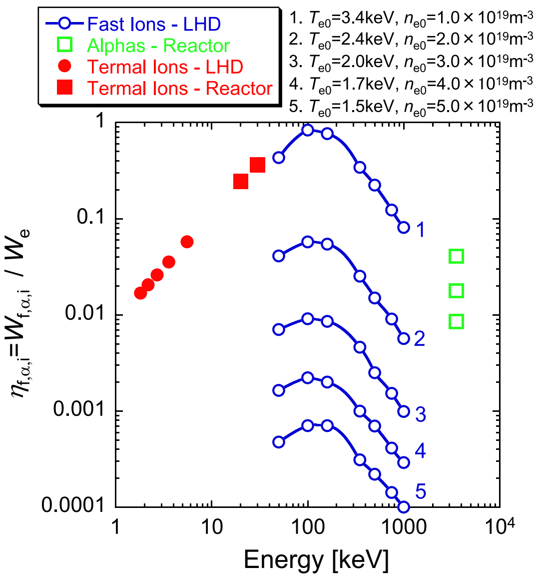


Fig. 2 Ratio of the effective contribution of energetic particles to pellet ablation against thermal electrons $\eta_{f,\alpha,i}$ versus their energy at $\rho = 0.6$ of the corresponding profiles.

lower velocity limit for the distribution function, respectively. The effective cross-section is written by $\Lambda = \hat{\sigma}_T + 3L(E)/2E$, where $\hat{\sigma}_T$ is the total cross-section for the elastic backscattering of electrons [9] and $L(E)$ [eV · m$^2$] is the energy loss function of the incident particles in the cloud, which is the fitted formula given by a semi-empirical cross-section for the discrete excitation, ionization, and dissociation processes. The energy loss function $L(E)$ for electrons [16], fast ions [21], and alpha particles [20] has a different energy range and energy-dependent function as shown in Fig. 1.

The ratio of the heat source in the cloud resulting from energetic particles against that from thermal electrons, $\eta_{f,\alpha,i} \equiv W_{f,\alpha,i}/W_e$, shows an effective contribution of energetic particles to pellet ablation since the heat source of the cloud $W$ is directly related to the ablation rate as $\dot{r}_{pel} \propto (W_{e*} + W_{f*})^{1/3}$ in the ablation model [19, 20], where the asterisk indicates the value at the sonic radius. In what follows, we assume $T_e = T_i$ and the thermal energy $E = 2T$.

The definitional equation $\eta_{f,i}$ is estimated by using the value at $\rho = 0.6$ of 1) the assumed electron density profiles (constant $n_e$ profiles with $n_{e0} = 1.0, 2.0, 3.0, 4.0, 5.0 \times 10^{19}\,\mathrm{m}^{-3}$), 2) the corresponding linear electron temperature profiles predicted by 1.5 times the ISS95 scaling [22], and 3) the density profiles of fast ions calculated by the FIT code [23] in LHD plasmas (at the NBI deposition power 10 MW). Under the present experimental conditions, LHD is a unique device that can experimentally demonstrate pellet ablation by fast ions since energetic NBI heating may affect the pellet ablation rate. The value of $\eta_\alpha$ is estimated by the value at $\rho = 0.6$ of the corresponding profiles under the condition of the fusion energy gain $Q = 5$ ($T_{e0} = 33$ keV, $n_{e0} = 1.0 \times 10^{20}\,\mathrm{m}^{-3}$) and $Q = 10$ ($T_{e0} = 23$ keV, $n_{e0} = 3.5 \times 10^{19}\,\mathrm{m}^{-3}$) in the International Thermonuclear Experimental Reactor (ITER) [24] and two cases ($T_{e0} = 22$ keV, $n_{e0} = 2.0 \times 10^{20}\,\mathrm{m}^{-3}$ and $T_{e0} = 27$ keV, $n_{e0} = 2.8 \times 10^{20}\,\mathrm{m}^{-3}$) in the Force Free Helical Reactor (FFHR) [25], while $\eta_i$ is also determined by the parameters of ITER. The value of $\eta_{f,\alpha,i}$ is a local parameter in target plasmas and the value at $\rho = 0.6$ is selected because it can be a representative parameter for ablation in both shallow and deep penetrations. Figure 2 shows the ratio of the effective contribution of energetic particles to the pellet ablation against thermal electrons $\eta_{f,\alpha,i}$ versus the energy of fast ions, alpha particles (3.5 MeV), and thermal ions.

The effect of fast ions on ablation cannot be neglected for low density, i.e. high temperature LHD plasmas because the heat flux of fast ions as a function of the slowing-down time increases with the electron temperature. Then large $q_f$ compensates small $q_e$ even though $\Lambda_f$ is smaller than $\Lambda_e$ (e.g., case 1 shown in Fig. 2). However, $\eta_f$ decreases with NBI injection energy, which results from the decline of $q_f$ by the decrement of $\Lambda_f$ at a certain NBI energy. In contrast, the effect of alpha particles on ablation is less than 10 % of that of thermal electrons in fusion reactors since $q_\alpha$ and $\Lambda_\alpha$ are always lower than those of electrons, supporting the fact that alphas slightly enhance the ablation rate in the calculation described in Ref. [20]. The effect of thermal ions cannot be neglected in fusion reactor plasmas, though it's not taken into account in major ablation models since the heat flux of thermal ions is lower and the energy loss is larger than that of electrons. In this estimation, it is found that the contribution of thermal ions to pellet ablation is significant for high temperature plasmas of several tens keV since $\Lambda_i$ exceeds $\Lambda_e$ at an energy of several keV. The inevitability of the application of NBI is not necessarily lost even in fusion plasmas due to needs for current drive and auxiliary heating leading to ignition. Accordingly, the effect of energetic ions on ablation must be assessed.

We have used the ABLATE code [19] to evaluate the effect of fast ions on pellet ablation. This code can deal with not only thermal electrons but also fast ions produced by NBI heating in regard to their role in ablation. It can also calculate the ablation rate profile (i.e., the pellet penetration depth) including the effect of non-time or time-dependent profiles of electron temperature and density during pellet ablation. The model is essentially extended from the NGS model [9] by the addition of the effect of fast ions. The attenuation of the energy of fast ions is newly expressed by the energy loss function of incident fast ions in the cloud $L_f(E_f)$ [21], while the solution of the Fokker-Planck equation for fast ions is used to calculate the energy and the heat flux of fast ions as seen in Eq. (4). The validity of this fast ion model was first demonstrated on the new region of the beam energy since NBI heated plasmas contain fast ions up to 180 keV in LHD. The analysis of pellet penetration depth using this code is discussed in Sec. 4.

## 3. Experimental Setup

The Large Helical Device (LHD) has a heliotron configuration which is composed of $l = 2/m = 10$ superconducting helical coils and three pairs of poloidal coils, and is superior to high density and steady state operations [12]. Its basic specifications include a nominal major radius of 3.9 m, an average minor radius of about 0.6 m, a plasma volume of 30 m$^3$, and a maximum magnetic field strength of ~ 3 T. Plasma heating is performed by three tangential neutral beam injection (NBI) systems all using a negative ion source [13]. The beam energy is 120 to 180 keV and the available total heating power is up to 13 MW. The electron temperature and density are measured by means of Thomson scattering [26] and an FIR interferometer [27], respectively.

Two pellet injectors (an in-situ pipe-gun pellet injector and a repetitive pellet injector) are installed in LHD. On the pipe-gun pellet injector, solid hydrogen pellets are produced in 8 barrels, and the pellet velocity and size are 1,000 to 1,200 m/s, with each cylinder being 3.0 mm in diameter and 3.0 mm in length (~$1 \times 10^{21}$ atoms) [14]. On the repetitive pellet injector, pellets are continuously formed and injected at a maximum repetition frequency of 11 Hz, and the pellet velocity and size are 300 to 700 m/s, with each cylinder being 2.5 mm in diameter and 2.5 mm in length (~$6 \times 10^{20}$ atoms) [15]. From both injectors, pellets are injected through the outer port of LHD into the plasmas by means of the pneumatic pipe-gun method using high pressure He gas. The pellet velocity is measured by the time-of-flight (TOF) which is a system that determines velocity based on the time difference of the pellet intersecting two pairs of laser-diodes and photodiodes about 1.8 m apart. The pellet mass is measured by the microwave cavity of the $TE_{103}$ mode [28] on the pipe-gun pellet injector. We conclude that the measurement deviation of the pellet velocity and mass are 0.3 - 1.4 % and ~5 %, respectively.

The measured penetration depth is determined based on the duration of $H_\alpha$ emissions measured from the backside of the pellet path and the assumption of a constant pellet velocity which is measured by TOF prior to the pellet injection into the plasmas. It has been previously confirmed that the pellet velocity during ablation in a plasma maintains its initial injection velocity; in other words, the radial pellet velocity is the same but the pellet velocity in the direction of the magnetic field line is accelerated by heating the pellet [29]. The duration of $H_\alpha$ emission, i.e., approximately the pellet lifetime, cannot be arbitrarily determined since the ergodic region is complex and the temperature and density in this area of LHD is unknown. Therefore, the start of pellet ablation is estimated based on the assumptions that the pellet ablates from the last closed flux surface of the vacuum magnetic configuration and that the pellet velocity is constant during the ablation, while the end of pellet ablation is determined by a sharp fall of the $H_\alpha$ signal. Ambiguity in penetration depth due to these assumptions is 0.5 - 7.5 cm including the measurement deviation of the pellet velocity and the scattering angle of pellet travel in the plasmas, while the plasma radius is about 0.85 to 0.98 m. Both the NBI heating condition and electron density before pellet injection are surveyed in the experiment, and neither ECH nor ICRH are used during the phase of pellet injection to document the effect of fast ions by NBI heating. In addition, pellets that penetrate beyond the magnetic axis are excluded (i.e., pellets of the penetration depth normalized by the minor radius $> 1$ are not considered) since electron temperature and density profiles change significantly when a pellet passes the plasma center.

## 4. Experimental Results

The results of a total of 52 discharges (129 datasets) in the pellet-fueled LHD experiments are included in order to analyze pellet penetration depth. The ranges of the LHD dataset are $T_{e0} = 0.76 - 3.43$ keV, $n_{e0} = 0.06 - 0.60 \times 10^{20}\ \mathrm{m}^{-3}$, $m_{pel} = 3.00 - 7.04 \times 10^{20}$ atoms, $v_{pel} = 212.89 - 1169.60$ m/s, $P_{dep} = 0.53 - 9.62$ MW, and $E_{NBI} = 104.94 - 174.64$ keV. The data include NBI Co-(12 %), Counter-(10 %), and Balance-(78 %) injection. The deposition power is 0.2 - 4.2 MW. Regression analysis is applied by the parameters of the NGS scaling $T_{e0}$, $n_{e0}$, $m_{pel}$, and $v_{pel}$ to investigate trend expressed in the LHD data. The regression expression for the penetration depth is the following formula (see Fig. 3 where RMSE = 0.029):

$$\lambda/a = 0.212 T_{e0}^{-0.685\pm0.027} n_{e0}^{-0.039\pm0.020} \times m_{pel}^{0.235\pm0.056} v_{pel}^{0.163\pm0.033}. \quad (5)$$

Normalization of the pellet penetration depth by the

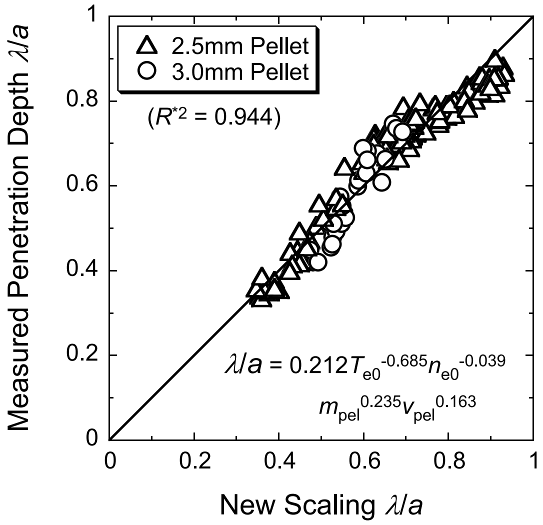


Fig. 3 The new scaling using the parameters of NGS scaling ($T_{e0}$, $n_{e0}$, $m_{pel}$, and $v_{pel}$) compared to the measured pellet penetration depth in LHD.

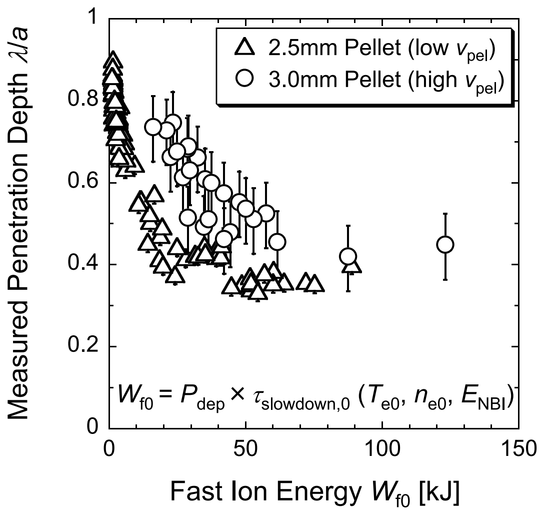


Fig. 4 The relationship between the measured pellet penetration $\lambda/a$ and the stored energy of fast ions $W_{f0}$ in pellet-fueled LHD discharges.

plasma radius, $\lambda/a = 1$, indicates that the pellet has reached the plasma center. Measured penetration depth is well expressed by Eq. (5). However, the standard error of the mean of the electron density $n_{e0}$ is not effective since the electron density $n_{e0}$ is strongly correlated with the electron temperature $T_{e0}$ and the deposition power $P_{dep}$ in the present data. Therefore, a new parameter is needed to describe the effect of fast ions in LHD plasmas.

The stored energy of fast ions in the plasma center is introduced as an indicator of the effect of fast ions on ablation,

$$W_{f0} = P_{dep} \times \tau_{slowdown,0}, \tag{6}$$

where $P_{dep}$ is the NBI deposition power in LHD plasmas and $\tau_{slowdown,0} \propto (T_{e0}^{3/2}/n_{e0}) \ln(1 + (E/E_{cr})^{3/2})$ is the

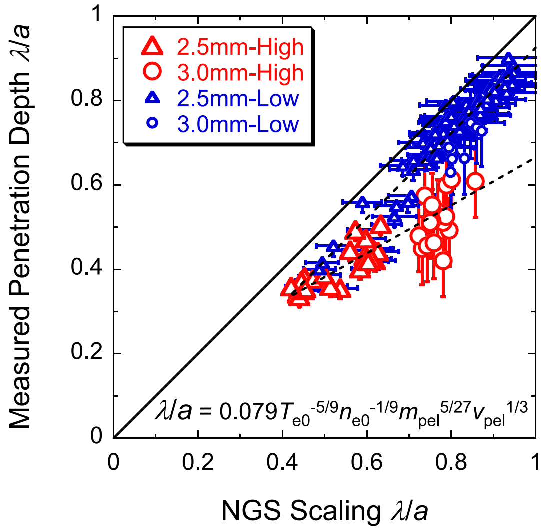


Fig. 5 NGS scaling considering only the effect of thermal electrons on the ablation compared to the measured pellet penetration depth at the same magnetic configuration ($R_{ax}$ = 3.6 - 3.7 m, $B_t \geq 2$ T).

slowing-down time at the plasma center. Figure 4 shows the distribution of data on the plane of the measured pellet penetration and the stored energy of fast ions in the pellet-fueled LHD discharges. The circle represents the 3-mm diameter pellet with fast pellet velocity on the pipe-gun pellet injector and the triangle is the 2.5-mm diameter pellet with slow pellet velocity on the repetitive pellet injector, as described in the previous section. The penetration depth becomes shallower with the increase of the energy of fast ions, and one can say that $\lambda/a$ correlates with $W_{f0}$. However, it should be noted that colinearity between $W_{f0}$ and $T_{e0}$ cannot be sufficiently excluded in the present database. The two curves composed of circles and triangles show the difference of the penetration depth due to the different pellet velocity and mass depending on the two injectors.

When one assumes linear profiles for the plasma electron temperature and density, Eq. (1) of the ablation rate in the NGS model becomes a scaling of penetration depth (NGS scaling), $\lambda/a = 0.079 T_{e0}^{-5/9} n_{e0}^{-1/9} m_{pel}^{5/27} v_{pel}^{1/3}$, where $\lambda/a$, $T_{e0}$, $n_{e0}$, $m_{pel}$, and $v_{pel}$ are the penetration depth normalized by the plasma minor radius, the central electron temperature, the central electron density, the pellet mass ($m_{pel} = (4/3)\rho_0 \pi r_{pel}^3 \times N_A$, where $\rho_0$ is the pellet material mass density and $N_A$ is the Avogadro's constant), and the pellet velocity, respectively [10]. The measured pellet penetration is compared with the NGS scaling which considers only the effect of thermal electrons on the ablation at the same magnetic configuration as that shown in Fig. 5. Here we define $W_{f0}/W_{dia} > 5\,\%$ as the high case and $W_{f0}/W_{dia} < 5\,\%$ as the low case, where $W_{dia}$ is the plasma stored energy. In the case of low $W_{f0}$, the trend agrees closely with the NGS scaling even for deep penetration, while also showing a slight offset from the NGS scaling. In contrast to this result, in the case of high $W_{f0}$

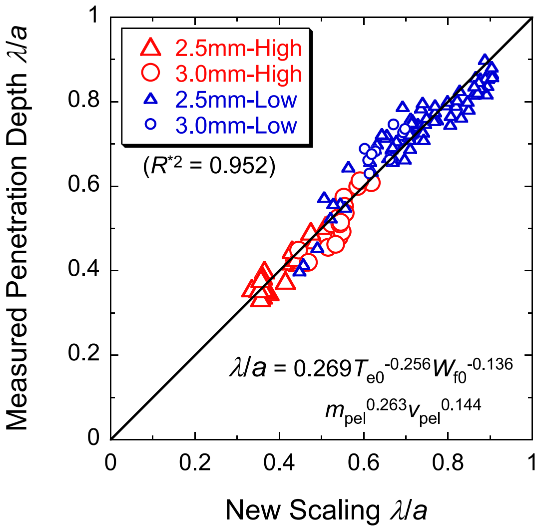


Fig. 6 New scaling using the stored energy of fast ions $W_{f0}$ instead of the electron density $n_{e0}$ compared to the measured pellet penetration depth in LHD.

the difference between measured and predicted pellet penetration is large for deep penetration although for shallow penetration there is no difference between the measured and predicted results in the two cases. The discrepancy of experimental results from NGS model suggests the effect of fast ions on pellet ablation since NGS scaling considers only thermal electrons. This tendency is pronounced when the pellet penetrates deeply and $W_{f0}$ is high. It is concluded that the experimental data produced from LHD cannot be expressed by NGS scaling alone.

In order to derive an empirical expression of the penetration depth, regression analysis was applied. The energy of fast ions $W_{f0}$ is used as a parameter in the statistical analysis since it has a potential to express the effect of fast ions on pellet ablation. The obtained regression expression is the following formula:

$$\lambda/a = 0.269T_{e0}^{-0.256\pm0.069}W_{f0}^{-0.136\pm0.024} \times m_{pel}^{0.263\pm0.047}v_{pel}^{0.144\pm0.030}. \quad (7)$$

As shown in Fig. 6 (RMSE = 0.026), the regression expression for the penetration depth accounts for the measured pellet penetration. The energy of fast ions $W_{f0}$ as a parameter is requisite to predict the measured penetration depth since the estimate value (i.e., the error bar of the multiplier factor) is smaller when the electron density $n_{e0}$ instead of $W_{f0}$ is used.

As described in Sec. 2, the new ABLATE code [19] is employed to analyze the pellet penetration depth in the LHD experiments. For this calculation, the fitting electron temperature and density profile based on experimental measurements using the Thomson scattering and the FIR interferometer, and the density profile of fast ions calculated by the FIT code [23] are used. The ABLATE code considering not only thermal electrons' but also fast ions' contribution to the ablation can calculate the ablation rate

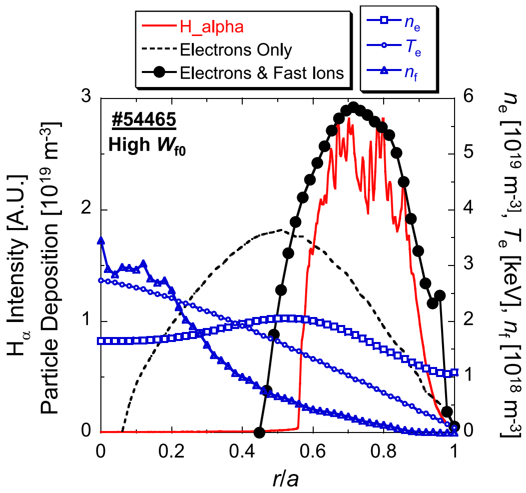


Fig. 7 $H_\alpha$ profile compared to the calculated ablation rate profile in the case of high $W_{f0}$ ($m_{pel}$ = 5.30 × $10^{20}$ atoms, $v_{pel}$ = 1129.70 m/s, and $W_{f0}$ = 42.12 kJ).

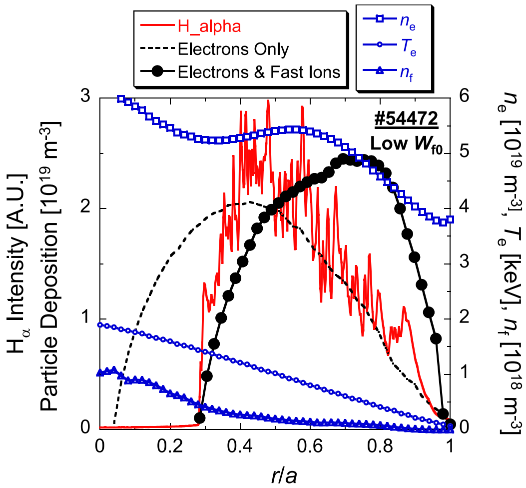


Fig. 8 $H_\alpha$ profile compared to the calculated ablation rate profile in the case of low $W_{f0}$ ($m_{pel}$ = 6.19 × $10^{20}$ atoms, $v_{pel}$ = 1148.40 m/s, and $W_{f0}$ = 16.14 kJ).

profile in Figs. 7 (for the high $W_{f0}$ case) and 8 (for the low $W_{f0}$ case), where the time-dependent profiles of the electron temperature and density during pellet ablation are considered in the calculation. The profile of $H_\alpha$ emission (solid lines), the model of electrons only (dashed lines), and the model of electrons and fast ions (filled circles) are compared. The measured pellet penetration depth is compared with the ABLATE penetration depth, i.e., the width of the calculated ablation rate profiles. Figure 9 shows a comparison between the ABLATE penetration depth considering only the ablation of thermal electrons and the measured penetration depth. This comparison duplicates the result from the NGS scaling shown in Fig. 5. A difference in the trends of the cases of high and low $W_{f0}$ is also observed. The comparison of the ABLATE penetration depth considering the ablation of thermal electrons and fast ions is shown in Fig. 10. The NGS scaling systematically un-

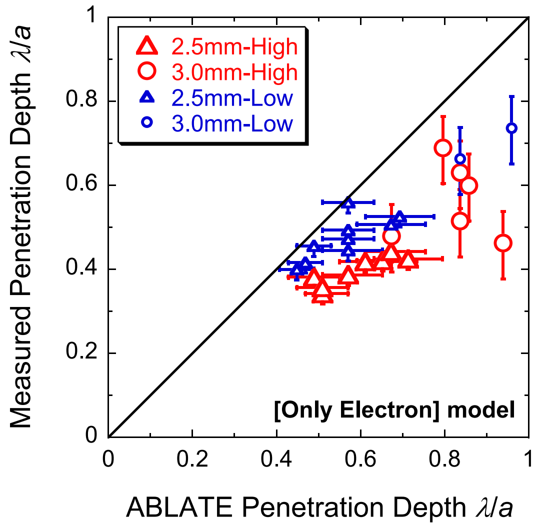


Fig. 9 ABLATE penetration depth considering only the ablation of thermal electrons compared to the measured penetration depth.

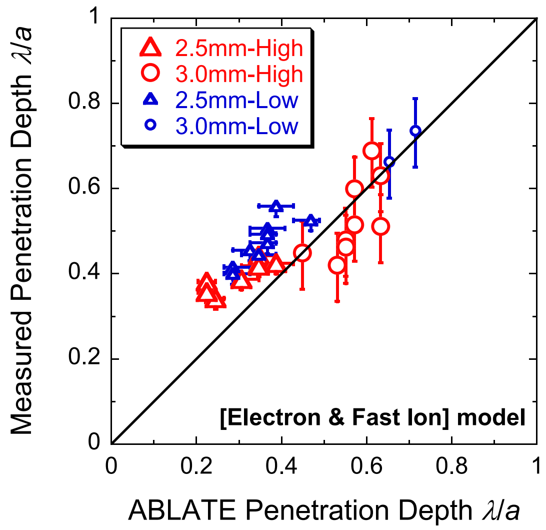


Fig. 10 ABLATE penetration depth considering the ablation of thermal electrons and fast ions compared to the measured penetration depth.

derestimates the penetration depth, which is pronounced in the case of high $W_{f0}$. Although the scattering is not reduced in the comparison with ABLATE, the correspondence between the experimental observation and the model calculation is improved. As well, deviation between the subsets (the high case of $W_{f0}/W_{dia} > 5\,\%$ and the low case of $W_{f0}/W_{dia} < 5\,\%$) is reduced. Penetration depths of the model including the effect of fast ions account for the experimental data.

## 5. Discussion

The IPADBASE [10] has been assembled to enable studies of pellet ablation theories that are used to describe the physics of pellet ablation in a tokamak plasma (JET,

Table 1 Plasma and pellet parameters in DIII-D, JET, and TFTR.

| Device | DIII-D | JET | TFTR |
|---|---|---|---|
| Data | 23 | 1 | 7 |
| $T_{e0}$ [keV] | 1.4-4.0 | 3.5 | 5.8-7.7 |
| $n_{e0}$ [$10^{20}$ m$^{-3}$] | 0.2-1.3 | 0.4 | 0.3-0.5 |
| $m_{pel}$ [$10^{20}$ atoms] | 1.1-20.1 | 15.1 | 14.6-35.1 |
| $v_{pel}$ [m/s] | 637-1178 | 1120 | 1054-2218 |
| $P_{dep}$ [MW] | 2.2-11.5 | 11.2 | 7.3-21.3 |
| $E_{NBI}$ [keV] | 70 | 80 | 110 |
| $W_{f0}$ [kJ] | 1.9-26.7 | 35.6 | 55.4-113.6 |

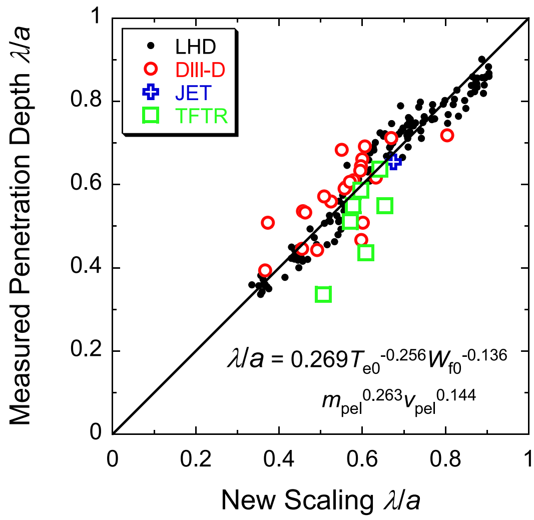


Fig. 11 New scaling compared to the measured pellet penetration depth on the combined pellet dataset (DIII-D, JET, and TFTR).

Tore Supra, DIII-D, FTU, TFTR, ASDEX Upgrade, JIPP T-IIU, RTP, and T-10). Data regarding NBI heated plasmas are selected as shown in Table 1. The data regarding TFTR have 5 - 10 times and two-times the pellet mass and velocity, respectively, than does LHD, and the data are identified as a case of high $W_{f0}$ as in the data of LHD because of energetic NBI heated plasmas ($E_{NBI}$ ~ 110 keV). The data regarding DIII-D and JET are very similar to LHD data except for the pellet mass and the NBI injection energy. These data are compared with the regression expression of the penetration depth expressed in Eq. (7) regarding LHD as shown in Fig. 11. DIII-D and JET data agree closely with the scaling, but the dataset from TFTR shows a trend different from that of LHD. The shapes of $T_e$ and $n_e$ profiles in the IPADBASE are linear/hollow for DIII-D, parabolic/parabolic for JET, and peaked/peaked for TFTR, respectively. In LHD experiments, these profiles are typically linear/flat or hollow, so the profile significantly varies among devices. Therefore, the scaling of the penetration depth might be improved by considering the dependence of these profiles.

The ABLATE code including the effect of fast ions on ablation can predict pellet penetration depth, as shown in Fig. 10. However, the shape and peak position of the pellet ablation rate profile differ from that of the measured $H_\alpha$ profile in Figs. 7 and 8. This distinction is especially significant in the case of low $W_{f0}$; consequently, the issue should be solved by the validation of $H_\alpha$ intensity based on the experimental observations of the ablation cloud and plasmoid. Thus, the model truly representing the experimental condition, i.e., the model that takes into consideration not only the neutral shielding cloud but also the plasmoid measured by LHD experiments [29], is required for comparison with the $H_\alpha$ radial profile under the same conditions. The other problem is a systematic underestimation of the penetration of the 2.5 mm pellets (represented in the figure by triangles). This might be improved by considering the shielding of the plasmoid treated in the neutral gas and plasma shielding (NGPS) model [30], which will take place in a future study.

# 6. Conclusion

Modeling of the penetration depth of the fueling pellet is prerequisite for establishing the optimal operational scenario of a fusion reactor. Penetration depth is closely related to fueling efficiency as well as to the impact on the parameters of the bulk plasma. Since the alpha particles play an essential role in heating the plasma in a fusion reactor, their effect on the ablation process of the injected pellet should be quantified. The present study has provided simulated experimental data describing this condition.

Pellet ablation in terms of pellet penetration depth has been studied under the condition of the presence of the fast ions produced by energetic NBI heating in LHD. We have introduced the stored energy of fast ions, $W_{f0}$, considering the effect of fast ions on pellet penetration depth. When $W_{f0}$ exceeds several percent of the total energy of the plasma as measured by diamagnetic diagnostics, the pellet penetration depth deviates significantly from the predicted value of the NGS model which treats only the ablation due to electrons. The dependence on $W_{f0}$ describes the effect of fast ions on ablation in LHD. When this expression is applied to the wider database (IPADBASE), a close agreement is found for DIII-D, whose plasma profile is similar to that of LHD. It is also verified in NBI heated plasmas in LHD that the ablation model including the effect of fast ions on ablation, the ABLATE code, can predict the observed penetration depth.

# Acknowledgements

The authors would like to thank the LHD technical staff for their encouragement and support. Dr. L.R. Baylor kindly made the data regarding IPADBASE available to the authors. We would also like to thank Dr. Y. Nakamura for his thoughtful suggestions on the revision of the ABLATE code and Dr. S. Murakami for his advise regarding the FIT code.

This work is supported by NIFS under Contract Nos. NIFS05ULPP521 and ULPP522.

[1] S.L. Milora, W.A. Houlberg *et al.*, Nucl. Fusion **35**, 657 (1995).
[2] D.K. Owens *et al.*, *Pellet Injection and Toroidal Confinement* (Proc. Tech. Comm. Mtg, Gut Ising, 1988), IAEA-TECDOC-534, IAEA, Vienna 191 (1989).
[3] G.L. Schmidt *et al.*, *1992 International Conference on Plasma Physics* (Proc. Conf. Innsbruck, 1992), Vol. 16C, Part I, European Physical Society, Geneva 255 (1992).
[4] P.T. Lang *et al.*, Nucl. Fusion **36**, 1531 (1996).
[5] R.D. Durst *et al.*, Nucl. Fusion **30**, 3 (1990).
[6] L.L. Lengyel, Nucl. Fusion **17**, 805 (1977).
[7] P.T. Lang *et al.*, Phys. Rev. Lett. **79**, 1487 (1997).
[8] S.L. Milora and C.A. Foster, IEEE Trans. Plasma Sci. **PS-6**, 578 (1978).
[9] P.B. Parks and R.J. Turnbull, Phys. Fluids **21**, 1735 (1978).
[10] L.R. Baylor *et al.*, Nucl. Fusion **37**, 445 (1997).
[11] B. Pégourié *et al.*, Plasma Phys. Control. Fusion **47**, 17 (2005).
[12] O. Motojima *et al.*, *IAEA Nucl. Fusion and Plasma Phys. 2004* (Vilamoura), paper OV/1-4.
[13] O. Kaneko *et al.*, Nucl. Fusion **43**, 692 (2003).
[14] H. Yamada *et al.*, Fusion Eng. Des. **49-50**, 915 (2000).
[15] H. Yamada *et al.*, Fusion Eng. Des. **69**, 11 (2003).
[16] W.T. Miles *et al.*, J. Appl. Phys. **43**, 678 (1972).
[17] S.L. Milora, Oak Ridge National Lab. Rep. ORNL/TM-8616 (1983).
[18] S. Sengoku *et al.*, *Plasma Phys. and Control. Nucl. Fusion Res.* (Proc. 10th Int. Conf. London, 1984), Vol. 1, IAEA, Vienna, 405 (1985).
[19] Y. Nakamura *et al.*, Nucl. Fusion **26**, 907 (1986).
[20] S.K. Ho and J. Perkins, Fusion Technol. **14**, 1314 (1988).
[21] H.H. Andersen and J.F. Ziegler, *Hydrogen Stopping Powers and Ranges in All Elements* (Pergamon Press, 1977).
[22] U. Stroth *et al.*, Nucl. Fusion **36**, 1063 (1996).
[23] S. Murakami *et al.*, Fusion Eng. Des. **26**, 209 (1995).
[24] ITER Physics Basis Editors *et al.*, Nucl. Fusion **39**, 2137 (1999).
[25] A. Sagara *et al.*, Fusion Eng. Des. **49-50**, 661 (2000).
[26] I. Yamada and K. Narihara, J. Plasma Fusion Res. **76**, 863 (2000).
[27] K. Kawahata *et al.*, Fusion Eng. Des. **34-35**, 393 (1997).
[28] M.J. Gouge *et al.*, Rev. Sci. Instrum. **61**, 2102 (1990).
[29] R. Sakamoto *et al.*, Nucl. Fusion **44**, 624 (2004).
[30] M. Kaufmann *et al.*, Nucl. Fusion **26**, 171 (1986).